The Bipolar Field-Effect Transistor: VII. The Unipolar Current Mode for Analog-RF Operation (Two-MOS-Gates on Pure-Base)*

Jie Binbin(揭斌斌)[1,†] and Sah Chih-Tang(薩支唐)[1,2,3,†]

(1 Peking University, Beijing 100871, China)
(2 University of Florida, Gainesville, Florida 32605, USA)
(3 Chinese Academy of Sciences, Foreign Member, Beijing 100864, China)

Abstract: This paper reports the DC steady-state current–voltage and conductance–voltage characteristics of a Bipolar Field-Effect Transistor (BiFET) under the unipolar (electron) current mode of operation, with bipolar (electron and hole) charge distributions considered. The model BiFET example presented has two MOS-gates on the two surfaces of a thin pure silicon base layer with electron and hole contacts on both edges of the thin base. The hole contacts on both edges of the thin pure base layer are grounded to give zero hole current. This 1-transistor analog-RF Basic Building Block nMOS amplifier circuit, operated in the unipolar current mode, complements the 1-transistor digital Basic Build Block CMOS voltage inverter circuit, operated in the bipolar-current mode just presented by us.

Key words: bipolar field-effect transistor theory; electron and hole contacts; electron emitter and collector; nMOS-BiFET

DOI: 10.1088/1674-4926/30/3/031001 **PACC:** 7340Q **EEACC:** 2560S; 2560B

1. Introduction

Conductivity modulation was first invoked by Lilienfeld 80 years ago in his three field-effect transistor (FET) patents filed in 1926 and 1928[1]. The unipolar FET was invented in 1952 by Shockley. He analyzed a FET structure using two facing reverse-biased p/n junctions on the two surfaces of a thin germanium sheet to change or gate the width of the conductive sheet hence the conductance modulation of the volume channel of the sheet by the two p/n junction gates[1]. The Complimentary Metal-Oxide-Silicon (CMOS) voltage inverter circuit was reported in 1963 by Wanlass, Sah and Moore[2,3] by connecting an unipolar p-surface-inversion-channel MOSFET in series with an unipolar n-surface-inversion-channel MOSFET. This CMOS inverter circuit has been the basic building block (BBB) circuit for digital integrated circuits. The unipolar surface-inversion-channel MOSFET has been the BBB of the small-signal analog and radio-frequency integrated circuits. These two BBB circuits are both present in mixed monolithic integrated circuits processing both digital and analog signals. Further advances of the integrated circuit technology aim at reducing the sizes of these two BBB circuits, including performing the multi-transistor circuit functions, such as the 2-transistor CMOS voltage inverter by one physical transistor.

It was recognized by us 24 months ago in March 2007 from the experimental data of nanometer MOS field-effect transistors[4,5] that eight current components can be simultaneously present in one physical field-effect transistor. These are: electron and hole channels, on the surface and in the volume of the semiconductor, and by diffusion and drift. To account for and to analyze these current components, we developed the analytical theory of the Bipolar Field Effect Transistor (BiFET) in two exactly equivalent mathematical representations: the electrochemical potential representation[6] which had provided us mathematically simplier analytical solution using single integrations, and the more conventional but mathematically more difficult drift and diffusion representation[7]. In our last month report (February 2009)[8], we described the physical realizations of the BiFET transistor and circuits[8]. In our next earlier report (November 2008)[9], we presented the mathematical analyses and gave the voltage–voltage, current–voltage, and power–voltage characteristics of the CMOS voltage inverter, realized in one physical BiFET transistor with two gates on a pure thin silicon base sheet. In this paper, we wish to report the calculated current–voltage and conductance–voltage characteristics of thin pure-base BiFETs under the unipolar (electron) current mode of operation, biased in the nMOS transistor configuration to serve as the one-transistor BBB small-signal analog and radio-frequency circuits for mixed signal monolithic silicon integrated circuits.

2. BiFET Theory for the Unipolar (Electron) Current mode

As shown in Figs. 1 and 2 of Ref. [8], repeated here as Fig. 1, the presence of the four contacts to the two edges of the

* This investigation and Jie Binbin have been supported by the CTSAH Associates (CTSA), founded by the late Linda Su-Nan Chang Sah, in memory of her 70th year.

† Corresponding authors. Email: bb_jie@msn.com and tom_sah@msn.com

Manuscript received 24 February 2009, revised manuscript received 28 February 2009

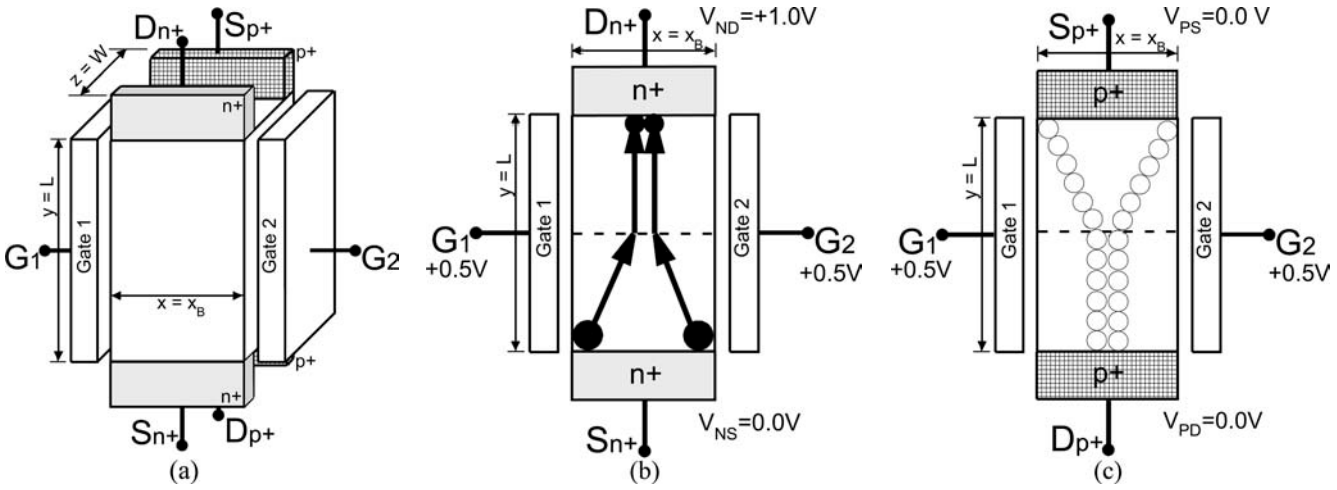

Fig. 1. Schematic diagram of the BiFET under Uni-Current (Electron Current Only) Operation. (a) The solid 3-dimensional view. (b) The electron concentration and the electron current density and trajectories in the two-section bias condition. (c) The hole concentration distribution, with no hole currents from grounding the two hole contacts, S_{p+} and D_{p+}.

pure-base layer of a Field-Effect Transistor with two MOS gates was the unique feature in the realization of a "complete" transistor. These four contacts are the source and drain (or sink) of electrons and holes. For our numerical computations, these electron and hole contacts at both edges ($y = 0$) and ($y = L$) of the base sheet or a rectangular thin base region or layer of the BiFET are assumed to cover the entire width and thickness of the two edges of the base layer so that both electron and hole surface and volume channels can be simultaneously present and conducting.

Under the bipolar current mode for the digital circuits such as the CMOS voltage inverter which we just reported[9], the electron drain (Dn+) and hole source (Sp+) contacts at the upper edge of the base are tied together by a metallic short circuit such as the interconnecting conductor metal, and the two tied contacts serve as the output terminal node. The DC power supply voltage is applied to the electrically isolated electron source (Sn+) and hole drain (Dp+) contacts at the lower edge of the base. In contrast, for this report on the unipolar (electron) current mode of operation for analog and RF circuits, the hole contacts Sp+ and Dp+ of the base are tied together by a metallic short circuit. This serves as the body terminal node or the transistor reference node. An alternative is to have one of the two p+ contacts electrically floating or not even present[8]. The resulting electrical characteristics are not expected to be very different, although small differences are strictly expected due to the difference in the spatial distribution of the holes at each bias point because of the different space locations of the hole source and hole drain or sink contacts to the thin pure base. The source voltage is applied to the electron contact (Sn+) at the bottom edge of the base, while the drain voltage is applied to the electron contact (Dn+) at the top edge of the rectangular base sheet. This nMOST bias configuration gives the following boundary conditions, (1) and (2), of the quasi-Fermi potentials or electrochemical potentials of the thin pure-base BiFET. In the mathematical analysis and numerical computations, all the potential variables, both internal and at the terminals, are normalized to the thermal voltage, k_BT/q, i.e. $U_N \triangleq qV_N/k_BT$, $U_P \triangleq qV_P/k_BT$ and $U_{IR} \triangleq qV_{IR}/k_BT$, where I is electric potential represented by the intrinsic Fermi potential, R=Reference potential node label, k_B=Boltzmann constant and T=lattice or thermal phonon temperature. Then, in the not-normalized notation, the nMOS boundary values are:

$$V_P(y = 0) = V_{BB} = 0, V_N(y = 0) = V_{SB}, \quad (1)$$

$$V_P(y = L) = V_{BB} = 0, V_N(y = L) = V_{DB}. \quad (2)$$

The DC electrical characteristics are governed by the three DC steady-state Shockley equations (Poisson and Electron and Hole Current Continuity Equations) with no electron-hole-generation-recombination-trapping. Simultaneous DC MOS transistor equations in the drift and diffusion (DD) representation were originally derived by us from the three Shockley equations[7]. The three assumptions in arriving at the analytical algebraic solutions necessary for providing precision benchmarks for gauging the accuracy of the compact models have been delineated but yet to be justified theoretically and numerically for a variety of device geometries and materials (or impurity concentrations and its spatial variations). They are subjects for future reports. These are: (i) the x-independence of the electron and hole electrochemical potentials, which leads to the decomposition of the two-dimensional transistor problem into one-dimensional equations in the base thickness direction or X-equations and one-dimensional equations in the base length direction or Y-equations, (ii) the constancy and near thermal equilibrium of the electron and hole mobilities and diffusivity, $D_n(x, y, z, t, V_N, V_P, V, T) \equiv D_n \equiv (k_BT/q)\mu_n$ for electrons and similarly for holes, and (iii) the omission of short-channel terms in both X-equations and Y-equations, which have the pre-factor $(L_D/L)^2$. These equations for a pure-base BiFET with the nMOS boundary values given by (1) and (2) are listed below with the integration of U from U_S to U_0 and X from 0 to X_B.

The Voltage Equation: (X-equation)

$$U_{GB} - U_S = \text{sign}(U_S - U_0) \times (C_D/C_O) \times [\exp(U_S - U_N) - \exp(U_0 - U_N) + \exp(U_P - U_S) - \exp(U_P - U_0)]^{1/2} \quad (3)$$

The Thickness Equation: (X-equation)

$$X_B = 2 \int \text{sign}(U - U_0) \partial_X U \times [\exp(U - U_N) - \exp(U_0 - U_N) + \exp(U_P - U) - \exp(U_P - U_0)]^{-1/2} \quad (4)$$

The Electron Current Equation: (Y-equation)

$$\begin{aligned} I_{DN} = {} & +kT\mu_n n_i L_D (W/L) \times \{ + \int (-P/n_i)(\partial U/\partial Y)\partial X && \text{bulk charge drift term} \\ & +(\partial/\partial Y)[(C_O/C_D) \times (2U_{GB} \times U_S - U_S^2] && \text{carrier space-charge drift term} \\ & +(\partial/\partial Y) \int (\partial U/\partial X)^2 \partial X\} && \text{transverse electric-field drift term} \\ & +qD_n n_i L_D (W/L) \times \{ - (\partial/\partial Y) \int (-P/n_i)\partial X && \text{bulk charge diffusion term} \\ & +(\partial/\partial Y)[(C_O/C_D) \times 2U_S]\} && \text{carrier space-charge diffusion term} \end{aligned} \quad (5)$$

The Hole Current Equation: (Y-equation)

$$I_{DP} = 0 \quad (6)$$

The notations here are defined in Ref. [7]. The zero value of the hole current, Equation (6), comes from the nMOS boundary values of the hole electrochemical potential: $U_P(Y = 0) = U_P(Y = 1) = 0$.

2.1. Flatband Boundary between the Two Sections

The rectangular base sheet or region of the BiFET is divided into two sections, a model first used by Shockley in 1952 for the volume-channel Junction-Gate FET, which was obviously following his 1949 idea on separating the bipolar junction transistor into three sections: collector/base/emitter[1,6]. We have called and shall continue to call these two sections the emitter section and the collector section[10,11]. The boundary between these two sections is a X–Z plane in a pure-base BiFET as shown in Figs. 1(b) and 1(c). Along this plane, the conduction and valence bands of the silicon are flat, and electron and hole concentrations are equal. So, on one side of this plane, electron concentration is always larger than hole concentration, while on the other side of the plane, electron concentration is always smaller than the hole concentration. This plane is called the flatband boundary plane separating the two sections. The Y-position, Y_0, of this plane or boundary surface, depends on the voltages applied to the six terminals of the pure-base Bipolar Field-Effect Transistor. One type of carriers (say electrons) flows through the surface channel in its emitter section, then, in the collector section, it would flow through the middle part of the base-region thickness, $x = x_0 = x_B/2$, or the volume channel in the collector region**.** This is schematically sketched in Figs. 1(b) for electrons and 1(c) for holes. It is important to note that the electron emitter section and hole collector section occupy the same physical space of the bipolar Field-Effect transistor, and the electron collector section and hole emitter section do also[11]. A most important feature, previously not noticed prior to our venture into the BiFET theory 24 month ago, is that the electron current and the hole current can simultaneously be presented in the same region or same physical space in the surface or volume regions of the base region.

Following Eq. (1) of Ref. [7], the Poisson Equation along this flatband plane can be written as follows:

$$[-(\partial^2 U/\partial X^2)_{Y=Y_0} - (L_D/L)^2(\partial^2 U/\partial Y^2)_{Y=Y_0}] = \{\exp[U_P(Y = Y_0) - U(X, Y = Y_0)] - \exp[U(X, Y = Y_0) - U_N(Y = Y_0)]\}/2. \quad (7)$$

Since the conduction and valence bands are flat along the X–Z plane boundary between the two sections, the normalized electric potential is given by $U(X, Y = Y_0) = U_{GB}$, which leads to $(\partial U/\partial X)_{Y=Y_0} = 0$ and $(\partial^2 U/\partial X^2)_{Y=Y_0} = 0$. The short-channel term $(L_D/L)^2(\partial^2 U/\partial Y^2)_{Y=Y_0}$ is dropped here, which is the subject of a later report. From the nMOS boundary values of (1) and (2), we have $U_P(Y = Y_0) = U_{BB} = 0$. Therefore, (7) gives:

$$U_N(Y = Y_0) = 2U_{GB}. \quad (8)$$

From the nMOS boundary values $U_N(Y = 0) = U_{SB}$, $U_N(Y = 1) = U_{DB}$, and noting that $U_N(Y = 0) \leqslant U_N(Y = Y_0) \leqslant U_N(Y = 1)$, it can be concluded that only when $U_{SB}/2 < U_{GB} < U_{DB}/2$, the base of the pure-base BiFET under the electron current mode of operation is divided into two sections.

2.2. One-Section Solution

For convenience of illustration without losing generality, we take the following two conditions. (i) The gate voltage, with the gate flatband voltage absorbed, is always larger than the non-negative source voltage, $U_{GB} > U_{SB} \geqslant 0$. (ii) The drain voltage is always not less than the source voltage, $U_{DB} \geqslant U_{SB}$. When the gate voltage is greater than one half of the drain voltage, $U_{GB} > U_{DB}/2$, an electron surface channel is formed in the whole base and the whole base region is the electron emitter, as discussed in the above subsection. When the gate voltage is equal to one half of the drain voltage,

$U_{GB} = U_{DB}/2$ the flatband plane ($Y = Y_0 = 1$) is located at the length or long end of the base sheet, $Y = 1$, but the whole base layer ($0 \leqslant X \leqslant X_B$, $0 \leqslant Y \leqslant 1$) is still the electron emitter. For convenience, $Y = 1$ is to be called here the drain end or edge. When the gate voltage is less than one half of the drain voltage, $U_{GB} < U_{DB}/2$, a hole surface channel is formed at the drain end. Then, the whole base layer is divided into two sections by the flatband plane ($Y = Y_0 < 1$): the electron emitter section ($0 < Y < Y_0$) and electron collector section ($Y_0 < Y < 1$).

The one-section solution assumes that the length of the electron collector can be neglected, and thus in any bias combinations of gate voltage and drain voltage, the whole base layer is always the electron emitter. So, the base-length modulation is not taken into account. Under this assumption, an effective drain voltage at the drain end, U_{Deff}, needs to be introduced:

$$U_{Deff} = U_{DB} \text{ when } U_{GB} \geqslant U_{DB}/2 \tag{9A}$$

$$U_{Deff} = U_N(Y = Y_0 < 1) = 2U_{GB} \text{ when } U_{GB} < U_{DB}/2. \tag{9B}$$

In the electron emitter, hole concentration is so small that both the bulk charge drift term and the bulk charge diffusion term in the electron current equation (5) can be dropped. Then, the following three current terms in the electron current are obtained:

$$\begin{aligned} I_{DN} = +kT\mu_n n_i L_D(W/L) \times \{ &+ (\partial/\partial Y)[(C_O/C_D) \times (2U_{GB} \times U_S - U_S^2] && \text{carrier space-charge drift term} \\ &+ (\partial/\partial Y) \textstyle\int (\partial U/\partial X)^2 \partial X\} && \text{transverse electric-field drift term} \\ +qD_n n_i L_D(W/L) \times \{ &+ (\partial/\partial Y)[(C_O/C_D) \times 2U_S]\} && \text{carrier space-charge diffusion term} \end{aligned} \tag{10}$$

Using Equation (67) in Ref. [7], the transverse electric-field drift term can be evaluated as follows:

$$\begin{aligned} \textstyle\int (\partial U/\partial X)^2 \partial X(X = 0 \text{ to } X_B) &= -2 \textstyle\int (\partial U/\partial X) \partial U && (U = U_0 \text{ to } U_S) \\ &= -2 \textstyle\int [\exp(U_S - U_N) - \exp(U_0 - U_N) + \exp(U_P - U_S) - \exp(U_P - U_0)]^{1/2} \partial U && (U = U_0 \text{ to } U_S) \end{aligned} \tag{11}$$

In order to make the algebra easy to follow, the following physical parameters are defined:
U_{00}, the mid-plane potential at the source end $Y = 0$.
U_{S0}, the surface potential at the source end $Y = 0$.

$$\begin{aligned} U_{GB} - U_{S0} = (C_D/C_O) \times [&\exp(U_{S0} - U_{SB}) \\ &- \exp(U_{00} - U_{SB}) + \exp(-U_{S0}) - \exp(-U_{00})]^{1/2} \end{aligned} \tag{12A}$$

$$\begin{aligned} X_B = 2 \textstyle\int \partial U \times [&\exp(U - U_{SB}) - \exp(U_{00} - U_{SB}) \\ &+ \exp(-U) - \exp(-U_{00})]^{-1/2}, \quad U = U_{00} \text{ to } U_{S0} \end{aligned} \tag{12B}$$

U_{01}, the mid-plane potential at the drain end $Y = 1$.
U_{S1}, the surface potential at the drain end $Y = 1$.
When $U_{GB} > U_{DB}/2$,

$$\begin{aligned} U_{GB} - U_{S1} = (C_D/C_O) \times [&\exp(U_{S1} - U_{DB}) \\ &- \exp(U_{01} - U_{DB}) + \exp(-U_{S1}) - \exp(-U_{01})]^{1/2} \end{aligned} \tag{13A}$$

$$\begin{aligned} X_B = 2 \textstyle\int \partial U \times [&\exp(U - U_{DB}) - \exp(U_{01} - U_{DB}) \\ &+ \exp(-U) - \exp(-U_{01})]^{-1/2}, \quad U = U_{01} \text{ to } U_{S1} \end{aligned} \tag{13B}$$

when $U_{GB} \leqslant U_{DB}/2$,

$$U_{01} = U_{S1} = U_{GB} \tag{13C}$$

I_{CP0}, the carrier space-charge parabolic drift component at the source end $Y = 0$.

$$I_{CP0} = kT\mu_n n_i L_D(W/L) \times (C_O/C_D) \times (2U_{GB} \times U_{S0} - U_{S0}^2) \tag{14}$$

I_{CP1}, the carrier space-charge parabolic drift component at the drain end $Y = 1$.

$$I_{CP1} = kT\mu_n n_i L_D(W/L) \times (C_O/C_D) \times (2U_{GB} \times U_{S1} - U_{S1}^2) \tag{15}$$

I_{TD0}, the transverse electric-field drift component at the source end $Y = 0$.

$$\begin{aligned} I_{TD0} = kT\mu_n n_i L_D(W/L) \times 2 \textstyle\int [&\exp(U - U_{SB}) \\ &- \exp(U_{00} - U_{SB}) + \exp(-U) - \exp(-U_{00})]^{1/2} \partial U, \\ &U = U_{00} \text{ to } U_{S0} \end{aligned} \tag{16}$$

I_{TD1}, the transverse electric-field drift component at the drain end $Y = 1$.
When $U_{GB} > U_{DB}/2$,

$$\begin{aligned} I_{TD1} = kT\mu_n n_i L_D(W/L) \times 2 \textstyle\int [&\exp(U - U_{DB}) \\ &- \exp(U_{01} - U_{DB}) + \exp(-U) - \exp(-U_{01})]^{1/2} \partial U, \\ &U = U_{01} \text{ to } U_{S1} \end{aligned} \tag{17A}$$

when $U_{GB} \leqslant U_{DB}/2$,

$$I_{TD1} = 0 \tag{17B}$$

I_{CL0}, the carrier space-charge linear diffusion component at the source end $Y = 0$.

$$I_{CL0} = qD_n n_i L_D(W/L) \times (C_O/C_D) \times 2U_{S0} \tag{18}$$

I_{CL1}, the carrier space-charge linear diffusion component at the drain end $Y = 1$.

$$I_{CL1} = qD_n n_i L_D(W/L) \times (C_O/C_D) \times 2U_{S1} \tag{19}$$

Integrating Equation (10) from $Y = 0$ to $Y = 1$, we obtain the one-section solution of the electron current of the pure-base

BiFET under the unipolar (electron) current mode of operation:

$$I_{DN1} = (I_{CP1} - I_{CP0}) + (I_{TD1} - I_{TD0}) + (I_{CL1} - I_{CL0}) \equiv I_{CP10} + I_{TD10} + I_{CL10}, \quad (20)$$

where I_{DN1} is the total drain electron current with the one-section assumption, I_{CP10} is the carrier space-charge parabolic drift component of the total current, I_{TD10} is the transverse electric-field drift component of the total current, and I_{CL10} is the carrier space-charge linear diffusion component of the total current.

2.3. Two-Section Solution

It is obvious that Equation (20) is exact when $U_{GB} \geqslant U_{DB}/2$ since there is only one section in the base region. When $U_{GB} < U_{DB}/2$, Equation (20) needs to be improved since there are two sections in the whole base region. In this bias range, Equation (10) is still valid in the electron emitter which covers the space of the base region from the source end $Y = 0$ to the flatband plane $Y = Y_0$. Integrating (10) from $Y = 0$ to $Y = Y_0$, the two-section solution of the electron current of the BiFET under the unipolar (electron) current mode of operation is obtained:

$$I_{DN2} \times Y_0 = I_{CP10} + I_{TD10} + I_{CL10}. \quad (21)$$

Next, the length of the electron collector, $1 - Y_0$, will be computed. Without recombination-generation centers in the base region and oxide-silicon interfaces, there are no electron sources and sinks in the base region, thus, the electron current must be continuous in the base, from the electron emitter to the electron collector. From the electrochemical potential representation[6], the electron current in the electron collector is given by:

$$I_{DN2} = qD_n(W/L) \times N_Y \times \partial U_N/\partial Y, \quad (22)$$

where N_Y is the total (area density) electron concentration at the position Y in the electron collector, $Y_0 \leqslant Y \leqslant 1$. The exact values of the total electron concentration at two special positions, N_0 at $Y = Y_0$ and N_1 at $Y = 1$, can be computed as follows:

$$N_0 = \int N(Y = Y_0)\mathrm{d}x = n_i \exp(U_{GB} - 2U_{GB}) \times x_B = n_i L_D \times \exp(-U_{GB}) X_B \quad (23)$$

$$N_1 = \int N(Y = 1)\mathrm{d}x = 2n_i L_D \int \exp(U - U_{DB})\partial U \times [\exp(U - U_{DB}) - \exp(U_{0D} - U_{DB}) + \exp(-U) - \exp(-U_{0D})]^{-1/2}, \quad U = U_{SD} \text{ to } U_{0D} \quad (24)$$

where $U_{SD} < U_{0D}$ in the electron collector

$$U_{GB} - U_{SD} = (C_D/C_O) \times (-1) \times [\exp(U_{SD} - U_{DB}) - \exp(U_{0D} - U_{DB}) + \exp(-U_{SD}) - \exp(-U_{0D})]^{1/2} \quad (25A)$$

$$X_B = 2 \int \partial U \times [\exp(U - U_{DB}) - \exp(U_{0D} - U_{DB}) + \exp(-U) - \exp(-U_{0D})]^{-1/2}, \quad U = U_{SD} \text{ to } U_{0D} \quad (25B)$$

As a first-order approximation, a linear variation of the total electron concentration in the electron collector region is assumed. In successive iterations, this initial approximation is removed.

$$N_Y \approx N_1 + (N_0 - N_1) \times (1 - Y)/(1 - Y_0). \quad (26)$$

Combining (22) and (26), and noting $U_N(Y = 1) = U_{DB}$ and $U_N(Y = Y_0) = 2U_{GB}$,

$$qD_n(W/L) \times \partial U_N = I_{DN2} \times [N_1 + (N_0 - N_1) \times (1 - Y)/(1 - Y_0)]^{-1} \times \partial Y$$

$$qD_n(W/L) \times (U_{DB} - 2U_{GB}) = I_{DN2} \times (1 - Y_0) \times \log_e(N_0/N_1)/(N_0 - N_1) \quad (27)$$

$$I_{DN2} \times (1 - Y_0) = qD_n(W/L) \times (U_{DB} - 2U_{GB}) \times (N_0 - N_1)/\log_e(N_0/N_1). \quad (28)$$

From (21) and (28), both I_{DN2} and Y_0 in the two-section voltage operation range $U_{GB} < U_{DB}/2$ are obtained. The value of Y_0 is set as one when $U_{GB} > U_{DB}/2$, $Y_0 = 1$, which means no electron collector, so that the two-section solution of the BiFET under the unipolar (electron) current mode of operation, Equation (21), covers all bias combinations of the gate voltage and the drain voltage. The deviation of the one-section solution from the two-section solution is as follows:

$$[(I_{DN1} - I_{DN2})/I_{DN2}] \times 100\% = -(1 - Y_0) \times 100\%. \quad (29)$$

3. Computed Current Voltage Characteristics

3.1. Characteristics from the One-Section Solution

Figures 2 and 3 show the physical parameters such as electric potential and electron current components in the pure-base BiFET under the unipolar (electron) current mode of operation, which is labeled in all figures as nMOS-BiFET, using the one-section solution. Figure 2 shows the mid-plane potential V_{01} and the surface potential V_{S1} at the drain end versus the gate voltage V_{GB} with the drain voltage V_{DB} varied. Both potentials rise linearly and then saturate with increasing gate voltage. Figure 3 shows the three electron current components at the drain end versus the gate voltage V_{GB} with the V_{DB} varied: the carrier space-charge parabolic drift components I_{CP1}, the absolute value of the transverse electric-field drift component $-I_{TD1}$ and the carrier space-charge linear diffusion component I_{CL1}. The I_{CP1} is two to three orders of magnitude larger than the I_{CL1} in the large gate voltage range. In the very large gate voltage range, the $-I_{TD1}$ has the same order of magnitude as the I_{CL1}, but with decreasing gate voltage, the $-I_{TD1}$ decreases much faster than exponentially and has a negligible value around $V_{GB} = V_{DB}$. The I_{CP1} versus V_{GB} and the I_{CL1} versus V_{GB} have the similar dependence on V_{DB}, while the $-I_{TD1}$

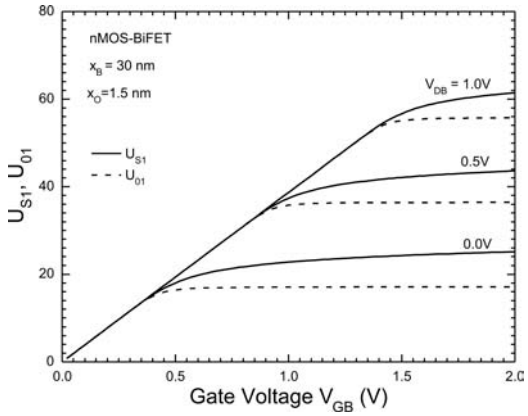

Fig. 2. Surface potential and mid-plane potential at the drain end of a pure-base BiFET under the unipolar (electron) current mode of operation, using the one-section solution.

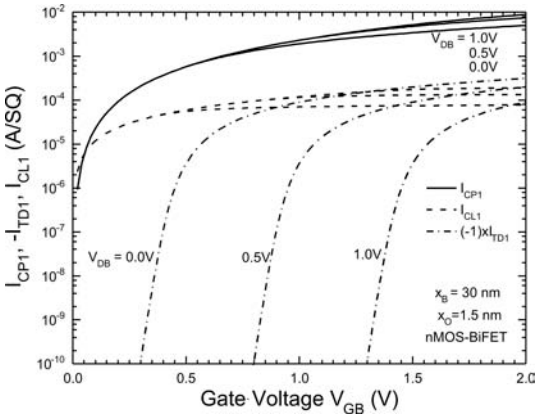

Fig. 3. Three electron current components at the drain end of a pure-base BiFET under the unipolar (electron) current mode of operation, using the one-section solution.

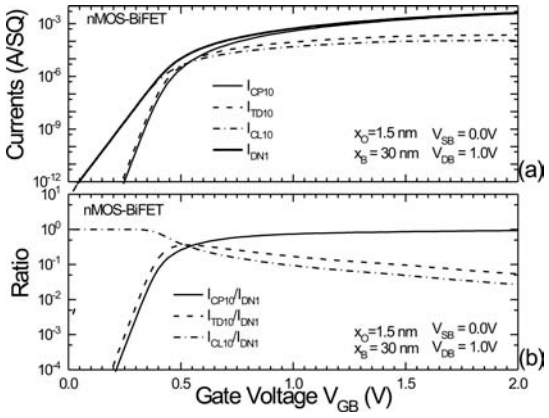

Fig. 4. Electron current and its three components of a pure-base BiFET under the unipolar (electron) current mode of operation versus gate voltage, using the one-section solution.

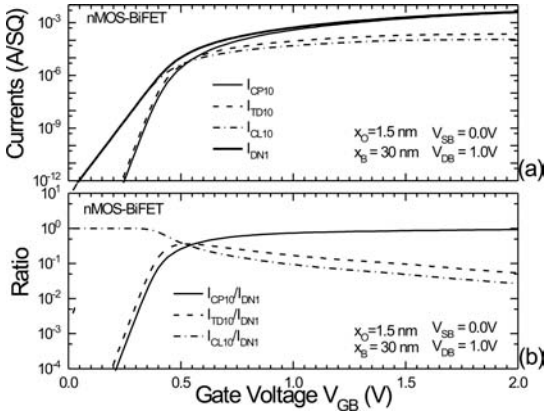

Fig. 5. Electron current and its three components of a pure-base BiFET under the unipolar (electron) current mode of operation versus drain voltage, using the one-section solution.

versus V_{GB} has much stronger dependence on V_{DB}, especially when V_{GB} is near V_{DB}.

Figures 4 and 5 give the transfer characteristics and drain output characteristics of the pure-base BiFET under the unipolar (electron) current mode of operations with the one-section assumption. Figures 4(a) and 5(a) show the total drain electron current and its drift and diffusion components. Figures 4(b) and 5(b) show the factional contribution to the total electron current I_{DN1} (or their ratios to the total electron current) of the carrier space-charge parabolic drift component I_{CP10}, the transverse electric-field drift component I_{TD10}, and the carrier space-charge linear diffusion component I_{CL10}. In the near-zero gate voltage range, the diffusion component I_{CL10} is dominant and several orders of magnitude larger than both the drift components I_{TD10} and I_{CP10}, while the I_{TD10} is one or two times larger than the I_{CP10}. In the very large gate voltage range (V_{GB} is around or larger than V_{DB}), the carrier space-charge parabolic drift component I_{CP10} is dominant and several orders of magnitude larger than both the transverse electric-field drift component I_{TD10} and the diffusion component I_{CL10}, while the I_{TD10} is one or two times larger than the I_{CL10}. In the middle gate voltage range (V_{GB} is near $V_{DB}/2$), the three current components are comparable to each other. It is important to note that the drain electron current saturation in the drain output characteristics comes from the mid-plane and surface potentials saturation.

3.2. Characteristics from the Two-Section Solution

Figures 6, 7 and 8 show the transfer characteristics of the nMOS-BiFET using the two-section solution, the total electron current I_{DN2} versus the gate voltage, and the length of the electron collector $(1 - Y_0)$ in the nMOS-BiFET versus the gate voltage. From Equation (29), the value $(1 - Y_0)$ also indicates the percentage difference between the one-section solution and the two-section solution. In Fig. 6, the drain voltage V_{DB} is varied. In Fig. 7 the base thickness x_B is varied. In Fig. 8, the gate oxide thickness x_O is varied. The drain voltage and the oxide thickness show significant impacts in the strong inversion gate voltage range, while the base thickness shows significant impact in the near-zero or subthreshold gate voltage range. As shown in these three figures, the electron collector length $(1 - Y_0)$ is near one at zero gate voltage, and it decreases exponentially with increasing gate voltage, and it is already a negligible value of 10^{-4} when $V_{GB} = 0.1$ V. This means that one-section solution is accurate enough when the gate voltage is larger than 0.1 V.

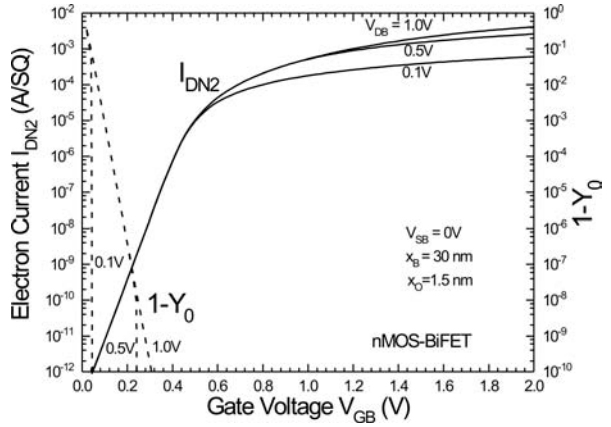

Fig. 6. Electron current and the electron collector length of a pure-base BiFET under the unipolar (electron) current mode of operation versus gate voltage, using the two-section solution, with V_{DB} varied.

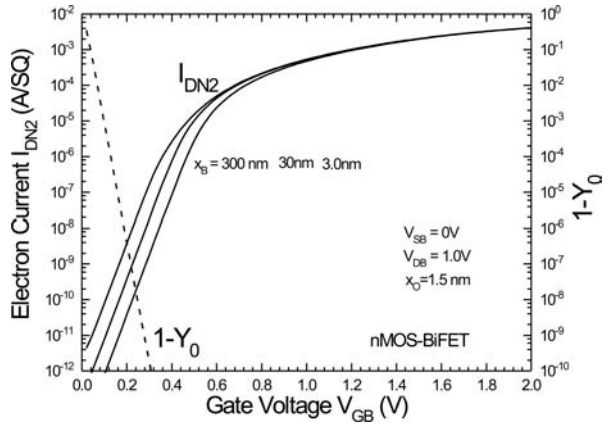

Fig. 7. Electron current and the electron collector length of a pure-base BiFET under the unipolar (electron) current mode of operation versus gate voltage, using the two-section solution, with X_{B} varied.

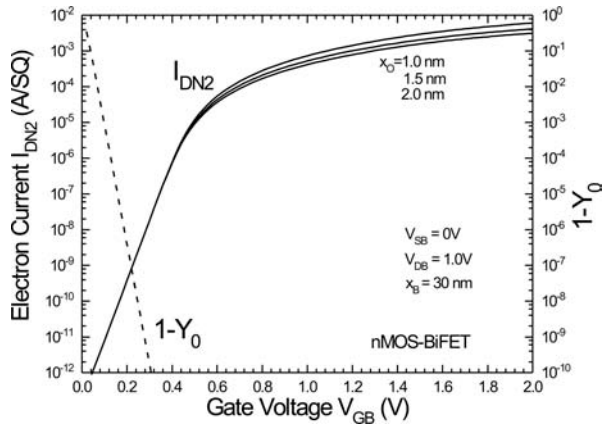

Fig. 8. Electron current and the electron collector length of a pure-base BiFET under the unipolar (electron) current mode of operation versus gate voltage, using the two-section solution, with X_{O} varied.

Figures 9 and 10 show the transconductance and drain conductance of the nMOS-BiFET using the two-section solution. In Figs. 9(a) and 9(b), the transconductance g_{m} and drain conductance g_{d} versus the gate voltage V_{GB} are plotted with the drain voltage V_{DB} varied. In Figs. 10(a) and 10(b), the transconductance g_{m} and drain conductance g_{d} versus the drain voltage V_{DB} are plotted with the gate voltage V_{GB} varied.

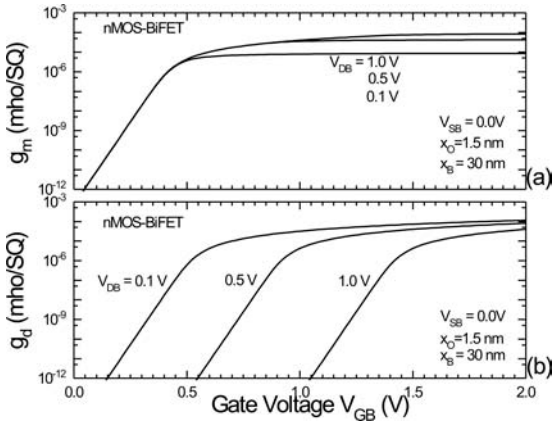

Fig. 9. Transconductance and drain conductance of a pure-base BiFET under the unipolar (electron) current mode of operation versus gate voltage, using the two-section solution.

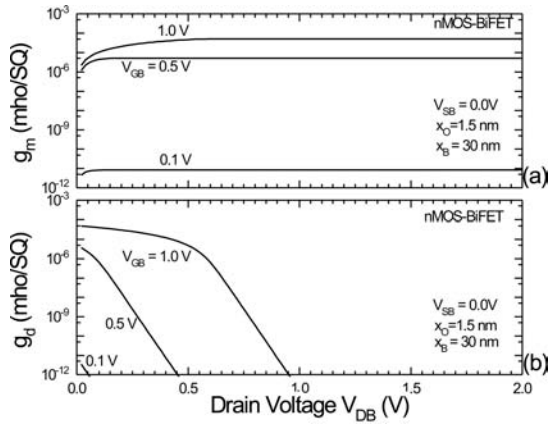

Fig. 10. Transconductance and drain conductance of a pure-base BiFET under the unipolar (electron) current mode of operation versus drain voltage, using the two-section solution.

They are very similar to the same characteristics of the single-gate bulk nMOSFET with a long surface inversion channel.

4. Summary

We have presented in this paper the current–voltage and conductance–voltage characteristics of the pure-base BiFET under the unipolar (electron) current mode of operation. The short channel longitudinal electric field gradient term is not taken into account, which is expected to be important in the pure-base transistor. The electron current of this nMOS-BiFET is given by both the one-section solution and two-section solution. In the practical operation bias range, the one-section solution gives nearly exact electron current in long channels.

Acknowledgment

We thank Professor Wang Yang-yuan of Peking University, Academician of Chinese Academy of Sciences, for his supports which have enabled us to undertake this study.

References

[1] Chih-Tang Sah, “Evolution of the MOS Transistor–from Con-

ception to VLSI," Proceedings of the IEEE, 76(10), 1280–1326, October, 1988. See text describing Figs. 1–3 for Lilienfeld's 1926–1928 patents of field effect transistors based on the conductivity modulation principle which he explicitly stated in the patents. See text description for reference [30] on Shockley's invention of the unipolar field-effect transistor based on conductance modulation via the volume channel thickness by the two p/n junction gate.

[2] Frank Wanlass and Chih-Tang Sah, "Nanowatt Logic Using Field-Effect Metal-Oxide Semiconductor Triodes," IEEE Solid-State Circuit Conference Proceedings, 32–33, February 20, 1963.

[3] Gordon E. Moore, Chih-Tang Sah, Frank Wanlass, "Metal-Oxide-Semiconductor Field-Effect Devices for Micropower Logic Circuitry," 41–55, in *Micropower Electronics*, Edited by Edward Keonjian, New York: Pergamon Press, 1964.

[4] Chih-Tang Sah and Bin B. Jie, "Double-Gate Thin-Base MOS Transistor: The Correct Theory," and Bin B. Jie and Chih-Tang Sah, "Double-Gate Thin-Base MOS Transistor: Characteristics for the Short Channel," Late-News Papers presented on May 23, 2007 at the Workshop on Compact Modeling (WCM2007) of the NSTI Nanotechnology Conference and Trade Show, May 22–24, 2007, hosted by the Nano Science and Technology Institute, Cambridge, MA02139, USA. http://www.nsti.org/Nanotech2007/WCM2007/.

[5] Chih-Tang Sah and Bin B. Jie, "Bipolar Theory of MOS Field-Effect Transistors and Experiments," Chinese J. Semiconductors, 28(10), 1497–1502, October, 2007.

[6] Sah Chih-Tang and Jie Binbin, "The Theory of Field-Effect Transistors: XI. The Bipolar Electrochemical currents (1-2-Gates on Thin-Thick Pure-Impure Base)," Journal of Semiconductors, 29(3), 397–409, March 2008.

[7] Jie Binbin and Sah Chih-Tang, "The Theory of Field-Effect Transistors: XII. The Bipolar Drift and Diffusion Currents (1-2-MOS-Gates on Thin-Thick Pure-Impure Base)," Journal of Semiconductors, 29(7), 1227–1241, July 2008.

[8] Sah Chih-Tang and Jie Binbin, "The Bipolar Field-Effect Transistor: XIII. Physical Realizations of the Transistor and Circuits (One-Two-MOS-Gates on Thin-Thick Pure-Impure Base)," Journal of Semiconductors, 30(2), 021001-1–12, February 2009.

[9] Jie Binbin and Sah Chih-Tang, "The Bipolar Field-Effect Transistor: VI. The CMOS Voltage Inverter Circuit (Two-MOS-Gates on Pure-Base)," Journal of Semiconductors, 29(11), 2079–2087, November 2008.

[10] Chih-Tang Sah and Bin B. Jie, "The Bipolar Field-Effect Transistor: II. Drift-Diffusion Current Theory (Two-MOS-Gates on Pure-base)," Chinese Journal of Semiconductors, 28(12), 1849–1859, December 2007.

[11] Jie Binbin and Sah Chih-Tang, "The Bipolar Field-Effect Transistor: III. Short Channel Electrochemical Current Theory (Two-MOS-Gates on Pure-Base)," Journal of Semiconductors, 29(1), 1–11, January 2008.